Structural Engineering and Mechanics, *Vol. 68, No. 4 (2018) 443-457*
DOI: https://doi.org/10.12989/sem.2018.68.4.443

Scattering of torsional surface waves in a three layered model structure

Shishir Gupta[a], Prasenjit Pati*, Anand Mandi[b] and Santimoy Kundu[c]

Department of Applied Mathematics, Indian Institute of Technology (Indian School of Mines), Dhanbad, India

(Received January 17, 2018, Revised September 29, 2018, Accepted October 3, 2018)

Abstract. In this article, a comparative study has been made to investigate the scattering behaviour of three layered structure model on torsional surface wave. For such model intermediate layer is taken as fiber reinforced composite, resting over a dry sandy Gibson substratum and underlying by different anelastic media. We consider two distinct mediums for topmost layer. In the first case, topmost layer has been taken as fluid saturated homogeneous porous layer, while in the second case the fluid saturated porous layer has been replaced by a transversely isotropic layer. Simple form expression for the secular equation of torsional surface wave has been worked out in both the cases by executing specific boundary conditions, which comprises Whittaker's function and its derivative, for imminent result that have been elaborated asymptotically. Some special cases have been constituted which are in excellent compliance with recorded literatures. For the sake of comparative study, numerical estimation and graphical illustration have been accomplished to identify the effects of the width ratio of the layers, Biot's gravity parameter, sandy parameter, porosity parameter and other heterogeneity parameters corresponding to the layers and half spaces, horizontal compressive and tensile initial stress on the phase velocity of torsional surface wave.

Keywords: torsional surface wave; transversely isotropy; porosity; fiber reinforcement; dry-sandy; secular equation

1. Introduction

In recent few decades, the study of earthquakes and seismic waves that move along the surface of earth and modeling upon surface wave propagation and interaction with layered anisotropic media is great challenge for both, theoretical and experimental seismologists and as well as researchers in the fields of geophysics, acoustics and non-destructive evaluation. Any disruption inside the earth may deliver as the initial cause for seismic wave generation. Among various types of seismic waves, torsional wave is one kind of surface wave that embroils circumferential displacement only, independent of the azimuthal angle. Being non-dispersive in nature, these are waves in which the particles of the strata twist clockwise and anticlockwise regarding the direction of motion of the waves. The supplement of torsional surface wave analysis and other surface wave propagation problems have been revealed by several researchers, due to their demolishing embezzlement abilities throughout earthquake and potential implementations in geophysical prospecting. In first of twentieth century Meissner (1921) has exhibited the existence of torsional surface wave in a heterogeneous elastic substrate with linear variation of the density and for shear moduli varying quadratically with depth. Bhattacharya (1975) has been explored the torsional wave propagation in a double-layered circular cylinder with imperfect bond. Extensive coverage and surveys on pertaining to surface waves can be found, for instance, in a monograph by Abo-El-Nour and Alsheikh 2009, Kakar and Kakar 2016, Lata *et al.* 2016, Manna *et al.* 2015, Ozturk and Akbarov 2009, Sharma and Kumar 2016, Singh *et al.* 2017, Son and Kang 2012, Sahu *et al.* 2018 and Vinh *et al.* 2016.

The inner structure of the earth is one of the crucial parameters to assess the seismic activity all over the world. Generally, a layered medium be formed of two or more material constituents connected at their interface in some fashion. The concepts of anisotropy, visco-elastic, fiber-composite, liquid filled poroelastic, transversely isotropic, elastic, plastic, sandy, granular, etc. in physical media have gained much attention in recent years. Some papers (Chattaraj *et al.* 2011, Chattopadhyay *et al.* 2009, Kumar *et al.* 2013, Islam *et al.* 2014, Watanabe 2014) can also be cited for their excellent contribution on the propagation of torsional waves in a elastic medium with various types of circumstance. Kakar (2015) studied the effect of rigid boundary on torsional wave transmission in an initially stressed heterogeneous elastic layer overlying an heterogeneous elastic half-space. Selim (2010) inquired into the torsional vibration in a single-walled carbon nanotubes under the effect of initial compression stresses. Torsional wave generation in a viscoelastic medium over an heterogeneous substratum under the effect of magnetic field was rendered by Kumari *et al.* (2016).

Manna *et al.* (2015) considered the impact of initial stress, anisotropy, reinforcement, and inhomogeneity on Love wave transference. Fiber-reinforced composite

*Corresponding author, Ph.D. Student
E-mail: prasenjitpati@gmail.com
[a]Professor
E-mail: shishir_ism@yahoo.com
[b]Ph.D. Student
E-mail: anand.mandi@gmail.com
[c]Assistant Professor
E-mail: kundu_santi@yahoo.co.in

ISSN: 1225-4568 (Print), 1598-6217 (Online)

medium are one class of composite medium in that the polymer matrix is reinforced by highly oriented polymer fibers, compose of fibers of high potency and modulus embedded in or bonded to a matrix with individual interfaces within them. In reality, the fibers might be nylon, boron, carbon, silicon carbide, or, conceivably, metal whiskers. Basically, the features of a fiber-reinforced composite confide dynamically on the direction of measurement, and hence, they are anisotropic materials. Thus, the modulus and tensile strength of a undirectionally aligned fiber-reinforced polymer are minimum when these characteristic are computed in the transverse direction of fibers and maximum value is perceived when they are computed in the longitudinal direction of fibers. Chaudhary *et al.* (2005) deliberated propagation of shear waves through a self-reinforced layer enclosed by two heterogeneous elastic semi-infinite media.

Biot (1962) was the first who devised the governing equations for surface wave propagation in poroelastic strata. A porous layer or a porous substance is a structure involving pores or voids. Vinh *et al.* (2016) discussed Rayleigh wave propagation in orthotropic fluid-saturated porous media. A porous material is very often distinguished by its porosity. Porous substances are envisaged precisely entirely in nature, in technology and in everyday life. Numerous natural elements suchlike various dense rocks, and soil (e.g., petroleum reservoirs, aquifers), biological tissues and several plastics, virtually all solid and semi-solid materials can be contemplated as porous media to varying degrees, usually consist of some fluid, such as water, air, oil or a mixture of miscellaneous fluids. Son and Kang (2012) performed shear wave propagation in a poroelastic layer sandwiched by two elastic media. Transversely isotropic material those elemental features that, plane of each strata is the plane of isotropy and the vertical axis is the axis of symmetry. Transversely isotropic solid associated with the class of hexagonal system, due to the circular symmetry around the hexagonal axis. This transverse plane has infinite planes of symmetry and thus among this plane, the material peculiarities are the same in every directions. Therefore, certain substances are also familiar as polar anisotropic substances. Kundu *et al.* (2017) remarkably studied shear waves in magneto-elastic transversely isotropic medium constrained between two inhomogeneous elastic layers.

Since earth is a gravitating medium, the force due to gravity, has a prominent significance in describing the static and dynamic complications of the earth. The reaction of gravity on wave propagation in an elastic solid media was first executed by Bromwich (1898), dealing the force of gravity as a category of body force. The phrase initial stress mentions to the stress subsisting in a body and not bounded by the operation of external forces. The influence of initial stresses on the transmission of torsional surface waves, emerged cause to natural incidence or through any artificial action is principally existent in the crustal layer as a effect of variation in temperature, external loading, atmospheric pressure, gravitation, weight dropping, overburden layer, slow process of creep, and largeness, can't be ignored. The works done by Ben-Hador and Buchen (1999), Carcione *et al.* (1988), Gupta *et al.* (2018), Shekhar and Parvez (2016) and Wang and Zhang (1998) can't be connivance as their endowments are adorable towards surface wave propagation.

Importance of initial stresses and gravitational forces in the mechanics of elastic solids and also understanding the subterranean response of surface wave generation in expressions of the material characteristic of the earth, geophysicsts and seismologists usually considered non homogeneous gravitating elastic models in semi infinite domains. Abo-El-Nour and Abo-Dahab (2008) explained the reflection and transmission of waves at the interface between magneto-viscoelastic materials subjected to the viscosity and the magnetic field. These ineluctable peculiarities and geophysical concepts towards the inward structure of the earth impelled the authors to examine the dispersion behaviour of torsional surface wave in a simple three layer model, consisting of a pre-stressed fiber reinforced layer overlying an pre-stressed gravitating dry sandy half space, whereas in the topmost layer for case–I, taken as pre-stressed fluid saturated porous and for case-II, it is pre-stressed transversely isotropic solid.

Due to notable applications in geophysical and geological fields such as soil dynamics, earthquake engineering, petroleum engineering, underwater acoustics and several subsurface geological inspection and exploration, and scheming miscellaneous civil engineering and marine structures such as dams, tunnels, bridges, highways, platforms and sub-surface development, the study of surface waves for inhomogeneous layered media over inhomogeneous half space has been of eminent attention to the theoretical and experimental seismologists, geophysicists and earth scientist. In present contribution, we study theoretically and analytically for obtaining secular equation of torsional wave generation incorporates determinating the solution of a partial differential equation or a system of partial differential modeling under admissible suitable boundary conditions. Variable separation technique is applied to obtained displacement components for mediums. Secular relation contains Whittaker function and its derivative where asymptotic expansion of Whittaker function and its derivatives has been accepted up to second order. The confined form of velocity equation has been obtained and some particular cases have been concluded by changing the thickness of the layers, reducing initial stress to be zero and by changing the inhomogeneity parameters of layers and half space. However, to our knowledge, a comparative study to shows an effect of the topmost layer of finite thickness on propagation of a torsional wave in a fiber reinforced medium of finite thickness lying on anisotropic gravitating dry-sandy infinite substratum have not been studied up till now. Comparative analysis has been carried out to examine and highlighting some significant peculiarities of the problem such as effect of initial stresses, width ratio of the layers, sandy parameter, porosity, reinforcement, Biot's gravity parameter and other heterogeneity parameters associated with layers and substratum on the common wave velocity of torsional surface wave.

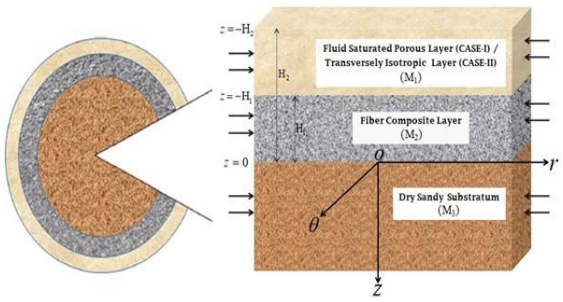

Fig. 1 Geometry of the problem

2. Formulation of the problem

We consider a medium consisting of a initially stressed fiber reinforced composite layer (M_2) of thickness H_1, resting on a initially stressed gravitating dry-sandy Gibson half space (M_3) and under an initially stressed anelastic layer (M_1) of thickness $(H_2 - H_1)$. Two different cases have been discussed. In case-I, we consider topmost layer (M_1) as a fluid saturated homogeneous porous layer where as in case-II, it has been taken as transversely isotropic layer. We consider cylindrical coordinate system (r, θ, z) in such a way that $r-$axis is in the direction of wave propagation and $z-$axis is taken in the direction of increasing depth and $z = 0$ is chosen as the interface between two layers, fiber reinforced layer (M_2), (occupies the region $-\infty < r < \infty,\ -\pi \le \theta < \pi,\ -H_1 \le z < 0$) and non-homogeneous anisotropic dry-sandy half space (M_3), (occupies the region $-\infty < r < \infty, 0 \le z$), where initial stress and rigidities vary linearly and also in the upper topmost layer (M_1) , (occupies the region $-\infty < r < \infty,\ -\pi \le \theta < \pi,\ -H_2 \le z < -H_1$) as shown in the Fig. 1.

3. Solution of the problem

3.1 Solution for the initially stressed topmost layer (M_1)

3.1.1 Solution for the initially stressed homogeneous fluid saturated porous layer (M_1), (for case -I)

The upper medium for case-I, is considered as fluid saturated homogeneous porous layer under initial stress. Ignoring the liquid viscosity and body force, dynamical equations for poroelastic medium subjected to initial stress P_{1F}, are stated by Biot (1962) as

$$\begin{aligned}
&\tau^{(1)}_{rr,r} + r^{-1}\tau^{(1)}_{r\theta,\theta} + \tau^{(1)}_{rz,z} + r^{-1}\left(\tau^{(1)}_{rr} - \tau^{(1)}_{\theta\theta}\right) - P_{1F}\omega_{\theta,z} \\
&= (\rho_{rr}u_r + \rho_{r\theta}U_r)_{,tt}; \\
&\tau^{(1)}_{r\theta,r} + r^{-1}\tau^{(1)}_{\theta\theta,\theta} + \tau^{(1)}_{\theta z,z} + 2r^{-1}\tau^{(1)}_{r\theta} - P_{1F}\omega_{z,r} \\
&= (\rho_{rr}v_\theta + \rho_{r\theta}V_\theta)_{,tt}; \\
&\tau^{(1)}_{rz,r} + r^{-1}\tau^{(1)}_{\theta z,\theta} + \tau^{(1)}_{zz,z} + r^{-1}\tau^{(1)}_{rz} - P_{1F}\omega_{\theta,r} \\
&= (\rho_{rr}w_z + \rho_{r\theta}W_z)_{,tt}
\end{aligned} \tag{1}$$

and

$$\begin{aligned}
&\tau_{,r} = (\rho_{r\theta}u_r + \rho_{\theta\theta}U_r)_{,tt};\ \tau_{,\theta} = (\rho_{r\theta}v_\theta + \rho_{\theta\theta}V_\theta)_{,tt}; \\
&\tau_{,z} = (\rho_{r\theta}w_z + \rho_{\theta\theta}W_z)_{,tt}
\end{aligned} \tag{2}$$

where $\tau^{(1)}_{ij}(i, j = r, \theta, z)$ = incremental stress components, (u_r, v_θ, w_z) = components of the displacement vector of the solid, (U_r, V_θ, W_z) = component of the displacement vector of the liquid and τ = stress vector due to liquid and

$$\begin{aligned}
&\omega_r = r^{-1}\left(w_{z,\theta} - rv_{\theta,z}\right)/2;\ \omega_\theta = \left(u_{r,z} - w_{z,r}\right)/2; \\
&\omega_z = r^{-1}\left((rv_\theta)_{,r} - v_{\theta,\theta}\right)/2
\end{aligned} \tag{3}$$

are components of the rotational vector ω and the 'comma' in the subscripts represents the partial differentiation with respect to the variables.

The porous medium constitutes volumetrically coupling solid-fluid aggregates; it may be modelled by the help of continuum porous media theories for both solid-matrix deformation and fluid flow so that the stress-strain relations for the liquid saturated anisotropic porous solids are

$$\begin{aligned}
\tau^{(1)}_{rr} &= (A_* + P_{1F})\varepsilon^{(1)}_{rr} + (A_* - 2N_1 + P_{1F})\varepsilon^{(1)}_{\theta\theta} \\
&\quad + (F_* + P_{1F})\varepsilon^{(1)}_{zz} + \Delta_\tau; \\
\tau^{(1)}_{\theta\theta} &= (A_* - 2N_1)\varepsilon^{(1)}_{rr} + A_*\varepsilon^{(1)}_{\theta\theta} + F_*\varepsilon^{(1)}_{zz} + \Delta_\tau; \\
\tau^{(1)}_{zz} &= F_*\varepsilon^{(1)}_{rr} + F_*\varepsilon^{(1)}_{\theta\theta} + C_*\varepsilon^{(1)}_{zz} + \Delta_\tau; \\
\tau^{(1)}_{r\theta} &= 2N_1\varepsilon^{(1)}_{r\theta};\ \tau^{(1)}_{\theta z} = 2L_1\varepsilon^{(1)}_{\theta z};\ \tau^{(1)}_{zr} = 2L_1\varepsilon^{(1)}_{zr}
\end{aligned} \tag{4}$$

where A_*, F_*, C_*, N_1 and L_1 = elastic constants of the medium, N_1 and L_1 = shear moduli of the anisotropic layer in the radial and the z-direction respectively, and the strains $\varepsilon^{(1)}_{ij}(i, j = r, \theta, z)$ are related by displacement components as

$$\begin{aligned}
&\varepsilon^{(1)}_{rr} = u_{r,r};\ \varepsilon^{(1)}_{\theta\theta} = r^{-1}v_{\theta,\theta} + r^{-1}u_r;\ \varepsilon^{(1)}_{zz} = w_{z,z}; \\
&\varepsilon^{(1)}_{zr} = \left(w_{z,r} + u_{r,z}\right)/2;\ \varepsilon^{(1)}_{r\theta} = \left(r^{-1}u_{r,\theta} + v_{\theta,r} - r^{-1}v_\theta\right)/2; \\
&\varepsilon^{(1)}_{\theta z} = \left(v_{\theta,z} + r^{-1}w_{z,\theta}\right)/2
\end{aligned} \tag{5}$$

Further, Δ_τ = the measure of interacting within the volume change of the solid and the liquid is a positive quantity. The relation between stress vector τ acting on the fluid phase of poroelastic material and the fluid pressure $\hat{P}^*$ can be described as

$$\tau = -\hat{\Theta}\hat{P}^* \tag{6}$$

where $\hat{\Theta}$ is the porosity of the poroelastic material. The mass coefficients $\rho_{rr}, \rho_{r\theta}$ and $\rho_{\theta\theta}$ are concerned with the densities $\hat{\rho}, \rho_s$ and ρ_f of the layer, the solid and the liquid systemically as

$$\rho_{rr} + \rho_{r\theta} = (1 - \hat{\Theta})\rho_s,\ \rho_{r\theta} + \rho_{\theta\theta} = \hat{\Theta}\rho_f \tag{7}$$

So, that aggregated mass density can be represents as

$$\hat{\rho} = \rho_{rr} + 2\rho_{r\theta} + \rho_{\theta\theta} = \rho_s + \hat{\Theta}(\rho_f - \rho_s) \tag{8}$$

Also, the mass coefficients fulfil the succeeding inequalities

$$\rho_{rr} > 0,\ \rho_{\theta\theta} > 0,\ \rho_{r\theta} < 0,\ \rho_{rr}\rho_{\theta\theta} - \rho_{r\theta}^2 > 0 \tag{9}$$

For the torsional surface wave along the radial direction, the mechanical displacement components for solid and liquid components are as following

$$\begin{aligned} &u_r = 0, v_\theta = v_{1F}(r,z,t), w_z = 0, \\ &U_r = 0, V_\theta = V_{1F}(r,z,t), W_z = 0 \end{aligned} \tag{10}$$

The above equation yield $\varepsilon_{\theta z}^{(1)}$ and $\varepsilon_{r\theta}^{(1)}$ strain components are non-zero and the other strain components will be zero. Therefore, useful stress-strain relations are

$$\tau_{\theta z}^{(1)} = 2L_1\varepsilon_{\theta z}^{(1)}, \tau_{r\theta}^{(1)} = 2N_1\varepsilon_{r\theta}^{(1)} \tag{11}$$

Now, Eq. (11) makes the Eqs. (1)-(2) as follows

$$\tau_{r\theta,r}^{(1)} + \tau_{\theta z,z}^{(1)} + 2r^{-1}\tau_{r\theta}^{(1)} - P_{1F}\omega_{z,r} = (\rho_{rr}v_{1F} + \rho_{r\theta}V_{1F})_{,tt} \tag{12}$$

and

$$(\rho_{r\theta}v_{1F} + \rho_{\theta\theta}V_{1F})_{,tt} = 0 \tag{13}$$

Using stress-strain relations of Eq. (4), Eq. (12) can be written as

$$\begin{aligned} &\left(N_1 - P_{1F}/2\right)\left(v_{1F,rr} - r^{-2}v_{1F} + r^{-1}v_{1F,r}\right) + \left(L_1 v_{1F,z}\right)_{,z} \\ &= (\rho_{rr}v_{1F} + \rho_{r\theta}V_{1F})_{,tt} \end{aligned} \tag{14}$$

From Eq. (13), let us assume $d^* = \rho_{r\theta}v_{1F} + \rho_{\theta\theta}V_{1F}$ i.e., $V_{1F} = \left(d^* - \rho_{r\theta}v_{1F}\right)/\rho_{\theta\theta}$

Now,

$$(\rho_{rr}v_{1F} + \rho_{r\theta}V_{1F})_{,tt} = \hat{d}v_{1F,tt} \tag{15}$$

where $\hat{d} = \rho_{rr} - \rho_{r\theta}^2/\rho_{\theta\theta}$.

Using Eq. (15) in Eq. (14), we get

$$\begin{aligned} &\left(N_1 - P_{1F}/2\right)\left(v_{1F,rr} - r^{-2}v_{1F} + r^{-1}v_{1F,r}\right) + \left(L_1 v_{1F,z}\right)_{,z} \\ &= \hat{d}\, v_{1F,tt} \end{aligned} \tag{16}$$

For the wave propagating along r - direction, the time harmonic solution of Eq. (16) can be assume as,

$$v_{1F} = \psi_{10}^{(1)}(z)J_1(kr)e^{i\omega t} \tag{17}$$

where the angular wave number k is expressed in terms of the angular velocity as $\omega(=ck)$; c is the phase velocity of the torsional surface waves; and $J_1(.)$ is the Bessel's function of first kind with order one.

Therefore, Eq. (16) can be presented as,

$$\frac{d^2\psi_{10}^{(1)}(z)}{dz^2} - k^2\left\{\left(N_1 - \frac{P_{1F}}{2}\right)\Big/L_1 - \kappa\hat{\rho}c^2/L_1\right\}\psi_{10}^{(1)}(z) = 0 \tag{18}$$

where $\kappa = \dfrac{\hat{d}}{\hat{\rho}} = \dfrac{1}{\hat{\rho}}\left(\rho_{rr} - \dfrac{\rho_{r\theta}^2}{\rho_{\theta\theta}}\right) = \phi_{11} - \dfrac{\phi_{12}^2}{\phi_{22}}$ is a non-dimensional parameter also $\phi_{11} = \rho_{rr}/\hat{\rho}$, $\phi_{12} = \rho_{r\theta}/\hat{\rho}$ and $\phi_{22} = \rho_{\theta\theta}/\hat{\rho}$ are non-dimensional parameter.

Inserting solution of Eq. (18) into Eq. (17) yields a single equation, giving displacement of upper fluid saturated homogeneous porous layer as

$$v_{1F}(r,z,t) = \left(Y_{11}e^{-\Omega_F z} + Y_{21}e^{\Omega_F z}\right)J_1(kr)e^{i\omega t} \tag{19}$$

where $\Omega_F^2 = k^2\left\{\left(N_1 - \dfrac{P_{1F}}{2}\right)\Big/L_1 - \kappa\left(\dfrac{c}{c_{1F}}\right)^2\dfrac{N_1}{L_1}\right\}$ and $c_{1F} = \sqrt{N_1/\hat{\rho}}$ is the shear wave velocity along the radial direction, corresponds to the initial stress free poroelastic layer and Y_{11} and Y_{21} are arbitrary constants.

3.1.2 Solution for initially stressed transversely isotropic layer (M_1), (for case -II)

The upper medium for case-II, is considered as transversely isotropic layer under initial stress. Assume u_*, v_* and w_* as the displacement components in radial, azimuthal, and axial directions, consequently for initially stressed transversely isotropic layer. In the layer, assuming that the torsional surface wave transmits in radial direction and that of all the mechanical properties related with it are not dependent of θ, so for torsional surface wave, $u_* = 0, v_* = v_{1T}(r,z,t)$ and $w_* = 0$.

The only non-vanishing equation of motion for initially stressed transversely isotropic layer is provided by Ding *et al.* (2006)

$$\tau_{r\theta,r}^{(2)} + \tau_{\theta z,z}^{(2)} + 2r^{-1}\tau_{r\theta}^{(2)} - P_{1T}\omega_{r\theta,r} = \rho_{1T}v_{1T,tt} \tag{20}$$

where P_{1T} is the initial stress acting along radial direction in layer and ρ_{1T} is the density of the layer and also $\omega_{r\theta} = v_{1T,r}/2$.

For transversely isotropic elastic medium the stiffness matrix are given as

$$\begin{pmatrix} \tau_{rr}^{(2)} \\ \tau_{\theta\theta}^{(2)} \\ \tau_{zz}^{(2)} \\ \tau_{\theta z}^{(2)} \\ \tau_{rz}^{(2)} \\ \tau_{r\theta}^{(2)} \end{pmatrix} = \begin{pmatrix} c_{11} & c_{12} & c_{13} & 0 & 0 & 0 \\ c_{12} & c_{11} & c_{13} & 0 & 0 & 0 \\ c_{13} & c_{13} & c_{33} & 0 & 0 & 0 \\ 0 & 0 & 0 & c_{55} & 0 & 0 \\ 0 & 0 & 0 & 0 & c_{55} & 0 \\ 0 & 0 & 0 & 0 & 0 & \dfrac{c_{11} - c_{12}}{2} \end{pmatrix} \begin{pmatrix} \varepsilon_{rr}^{(2)} \\ \varepsilon_{\theta\theta}^{(2)} \\ \varepsilon_{zz}^{(2)} \\ 2\varepsilon_{\theta z}^{(2)} \\ 2\varepsilon_{rz}^{(2)} \\ 2\varepsilon_{r\theta}^{(2)} \end{pmatrix} \tag{21}$$

where $\tau_{ij}^{(2)}(i,j = r,\theta,z)$ = stress components, c_{11}, c_{12}, c_{13}, c_{33}, c_{55} = elastic constant, $\varepsilon_{ij}^{(1)}(i,j = r,\theta,z)$ = strain components and the conditions of existence for a transversely isotropic medium are

$c_{11}^2 > c_{12}^2,\ (c_{11} + c_{12})c_{33} > 2c_{13}^2,\ c_{55} > 0$

and nonzero strain components related to the displacement component v_{1T} by

$$\varepsilon_{r\theta}^{(2)} = \left(v_{1T,r} - r^{-1}v_{1T}\right)/2,\ \varepsilon_{\theta z}^{(2)} = v_{1T,z}/2 \tag{22}$$

Using Eq. (22) and Eq. (21) in Eq. (20) we get,

$$\begin{aligned}&\left(c_{11}-c_{12}-P_{1T}\right)v_{1T,rr} + \left(c_{11}-c_{12}\right)\left(r^{-1}v_{1T,r} - r^{-2}v_{1T}\right)\\ &+2c_{55}v_{1T,zz} = 2\rho_{1T}v_{1T,tt}\end{aligned} \tag{23}$$

We assume the harmonic wave solution with amplitude of displacement as a function of depth may be taken as $v_{1T} = \psi_{20}^{(2)}(z)J_1(kr)e^{i\omega t}$; which lead Eq. (23) to

$$\frac{d^2\psi_{20}^{(2)}}{dz^2} - \Omega_T^2\psi_{20}^{(2)} = 0 \tag{24}$$

where $\Omega_T^2 = k^2\left[\begin{array}{l}\dfrac{\left(c_{11}-c_{12}\right)}{k^2}\left\{\dfrac{1}{2r^2c_{55}} - \dfrac{kJ_1'(kr)}{2rc_{55}J_1(kr)}\right\}\\ -\dfrac{\left(c_{11}-c_{12}-P_{1T}\right)J_1''(kr)}{2c_{55}J_1(kr)} - \dfrac{c^2}{c_{1T}^2}\end{array}\right]$

and $c_{1T} = \sqrt{c_{55}/\rho_{1T}}$ is the shear wave velocity in the medium, and the 'dash' in the superscripts denotes the differentiation with respect to the variables.

Inserting solution of Eq. (24), giving the displacement for torsional wave in the upper transversely isotropic layer with the axis of symmetry coinciding with the vertical axis as

$$v_{1T}(r,z,t) = \left(Y_{12}e^{-\Omega_T z} + Y_{22}e^{\Omega_T z}\right)J_1(kr)e^{i\omega t} \tag{25}$$

where Y_{12} and Y_{22} are arbitrary constants.

3.2 Solution for intermediate initially stressed fiber-reinforced composite layer (M_2)

The Cauchy's stress tensor in fiber-reinforced linearly elastic anisotropic model with preferred direction $\hat{\varsigma} = (\varsigma_1, \varsigma_2, \varsigma_3)$, are given by Spencer (1972) may be written as,

$$\begin{aligned}\bar{\sigma}_{ij} &= \tilde{d}\sum_{k=1}^{3}\bar{e}_{kk}\delta_{ij} + \tilde{a}\left(\sum_{k=1}^{3}\sum_{m=1}^{3}\varsigma_k\varsigma_m\bar{e}_{km}\delta_{ij} + \sum_{k=1}^{3}\bar{e}_{kk}\varsigma_i\varsigma_j\right)\\ &+2f_T\bar{e}_{ij} + 2\left(f_L - f_T\right)\left(\varsigma_i\sum_{k=1}^{3}\varsigma_k\bar{e}_{kj} + \varsigma_j\sum_{k=1}^{3}\varsigma_k\bar{e}_{ki}\right)\\ &+\tilde{b}\left(\varsigma_i\varsigma_j\sum_{k=1}^{3}\sum_{m=1}^{3}\varsigma_k\varsigma_m\bar{e}_{km}\right);\ i,j = r,\theta,z\end{aligned} \tag{26}$$

where $\bar{\sigma}_{ij}$ = stress components, δ_{ij} = Kronecker delta, $\bar{e}_{ij}\left\{=\left(\bar{u}_{j,i} + \bar{u}_{i,j}\right)/2\right\}$ = components of infinitesimal strain, $\bar{u}_j$ = displacement components, ς_i = components of $\hat{\varsigma}$, such that $\sum\varsigma_i^2 = 1$; $\tilde{d},\ f_T, \tilde{a}, \tilde{b}$ and $\left(f_L - f_T\right)$ = elastic constants with dimensions of stress.

The shear modulus in longitudinal shear in the preferred direction is identified as f_L, and the shear modulus in transverse shear across the preferred direction is identified as f_T. $\tilde{a}$ and $\tilde{b}$ are the specific stress components to take into account in different layers of the concrete part of the composite material.

In Eq. (26), the unit vector $\hat{\varsigma}$ gives the orientation of the family of fibers in axial (z), azimuthal (θ), and radial (r), directions, respectively. Setting the component $\varsigma_2 = 0$, gives the orientation of one's choice, so assuming that, the fibers are initially lie in the surface for some fixed value of θ, at an angle υ to the radial axis. Therefore, the components of vector $\hat{\varsigma}$ in the cylindrical polar coordinate system are $\hat{\varsigma} = (\varsigma_1, \varsigma_2, \varsigma_3) = (\sin\upsilon, 0, \cos\upsilon)$. For torsional surface waves propagating along radial direction and causing displacement in an azimuthal direction only, we have the following displacement components

$$\bar{u}_r = 0, \bar{u}_\theta = v_2(r,z,t), \bar{u}_z = 0 \tag{27}$$

In view of Eq. (27), strains are associated with displacements by the subsequent relations

$$\begin{aligned}&\bar{e}_{rr} = 0, \bar{e}_{zz} = 0, \bar{e}_{\theta\theta} = 0, \bar{e}_{rz} = 0,\\ &\bar{e}_{r\theta} = \left(v_{2,r} - r^{-1}v_2\right)/2, \bar{e}_{\theta z} = v_{2,z}/2\end{aligned} \tag{28}$$

Using Eq. (28) and Eq. (27) in Eq. (26), one may get the succeeding non-zero stress components

$$\begin{aligned}&\bar{\sigma}_{\theta z} = \tilde{R}v_{2,z} + \tilde{Q}\left(v_{2,r} - r^{-1}v_2\right);\\ &\bar{\sigma}_{r\theta} = \tilde{S}\left(v_{2,r} - r^{-1}v_2\right) + \tilde{Q}v_{2,z}\end{aligned} \tag{29}$$

where

$$\begin{aligned}&\tilde{S} = f_T + \left(f_L - f_T\right)\varsigma_1^2, \tilde{R} = f_T + \left(f_L - f_T\right)\varsigma_3^2,\\ &\tilde{Q} = \left(f_L - f_T\right)\varsigma_1\varsigma_3\end{aligned} \tag{30}$$

Hence, by the properties of torsional wave, we are left the only one characteristic equation of motion for the generation of a torsional wave in absentia of body force is obtained as

$$\bar{\sigma}_{r\theta,r} + r^{-1}\bar{\sigma}_{\theta\theta,\theta} + \bar{\sigma}_{\theta z,z} + 2r^{-1}\bar{\sigma}_{r\theta} - \left(\bar{P}\bar{e}_{z\theta}\right)_{,z} = \bar{\rho}v_{2,tt} \tag{31}$$

where $\bar{P}(z) = P_2$ is the initial stress along radial direction and $\bar{\rho}(z) = \rho_2$ is density of the fiber reinforced medium.

Substituting Eq. (29) and Eq. (30), in Eq. (31) becomes

$$\begin{aligned}&\tilde{S}v_{2,rr} + 2\tilde{Q}v_{2,rz} + \left(\tilde{R} - P_2/2\right)v_{2,zz} + r^{-1}\tilde{S}v_{2,r} + r^{-1}\tilde{Q}v_{2,z}\\ &-r^{-2}\tilde{S}v_2 = \rho_2 v_{2,tt}\end{aligned} \tag{32}$$

Assuming the time harmonic solution, the displacement of wave along radial direction in the medium may be examined of the form

$$v_2 = \psi_{20}(z)J_1(kr)e^{i\omega t} \tag{33}$$

Using Eq. (33) in Eq. (32), can be express as

$$\frac{d^2\psi_{20}(z)}{dz^2} + \tilde{M}\frac{d\psi_{20}(z)}{dz} + \tilde{E}\psi_{20}(z) = 0 \tag{34}$$

where

$$\tilde{E}=\tilde{S}\left(\frac{k^2J_1''(kr)}{J_1(kr)}+\frac{kJ_1'(kr)}{rJ_1(kr)}+\frac{\rho_2\omega^2}{\tilde{S}}-\frac{1}{r^2}\right)\Big/\left(\tilde{R}-\frac{P_2}{2}\right),$$

$$\tilde{M}=\tilde{Q}\left(\frac{2kJ_1'(kr)}{J_1(kr)}+\frac{1}{r}\right)\Big/\left(\tilde{R}-\frac{P_2}{2}\right),\quad\text{and}\quad c_2=\sqrt{f_T/\rho_2}$$ is the shear wave velocity in reinforced medium along radial direction.

Therefore, the displacement for initially stressed fiber reinforced medium in view of Eq. (34) is considered periodic form as

$$v_2(r,z,t)=e^{-\tilde{M}z/2}\left(Y_3\sin(qz)+Y_4\cos(qz)\right)J_1(kr)e^{i\omega t}\quad(35)$$

where $q^2=\tilde{E}-\tilde{M}^2/4,\tilde{M},\tilde{E},Y_3$ and Y_4 are constants.

3.2 Solution for initially stressed gravitating dry-sandy Gibson half space (M_3)

The constitutive equations of motion for dry sandy half space under influence of gravity and initially stressed and in the nonappearance of body forces, can be written from Biot (1966), as

$$\begin{aligned}&\hat{\pi}_{r\theta,r}+\hat{\pi}_{z\theta,z}+2r^{-1}s_{r\theta}+\left\{\left(\hat{P}-\hat{\rho}gz\right)\ell_{z\theta}\right\}_{,z}\\&-\hat{\rho}gz\left\{\left(v_{,r}+r^{-1}v\right)/2\right\}_{,r}=\rho v_{,tt}\end{aligned}\quad(36)$$

where $v=v_3(r,z,t)$ is the displacement component along the azimuthal direction, $\hat{P}$ = initial stress along radial direction and $\hat{\rho}$ = density of the medium.

In the dry sandy Gibson half space, disparity of directional rigidity, initial stress and density have been taken as

$$\mu=\mu_3(1+\alpha z),\hat{\rho}=\rho_3,\hat{P}=P_3(1+\beta z)\quad(37)$$

The stress-strain-displacement relations (non-zero) for the sandy half space are

$$\begin{aligned}&\hat{\pi}_{r\theta}=2T\ell_{r\theta};\hat{\pi}_{z\theta}=2T\ell_{z\theta};\\&\ell_{r\theta}=\left(v_{3,r}-r^{-1}v_3\right)/2;\ell_{z\theta}=v_{3,z}/2\end{aligned}\quad(38)$$

Further $T=\eta\mu$, where η is the sandy parameter and μ is the modulus of rigidity.

Using above relations in Eq. (36) we have

$$\begin{aligned}&(\eta\mu(z)-\hat{\rho}gz/2)\left(v_{3,rr}+r^{-1}v_{3,r}-r^{-2}v_3\right)\\&+\left\{\eta\mu(z)+(\hat{P}(z)-\hat{\rho}gz)/2\right\}v_{3,zz}\\&+\left\{\eta\mu'(z)+(\hat{P}'(z)-\hat{\rho}g)/2\right\}v_{3,z}=\hat{\rho}v_{3,tt}\end{aligned}\quad(39)$$

For a harmonic wave propagating along radial direction we execute solution of Eq. (36) as

$$v_3=\psi_{30}(z)J_1(kr)e^{i\omega t}\quad(40)$$

where, $\psi_{30}(z)$ is the solution of

$$\begin{aligned}&\frac{d^2\psi_{30}(z)}{dz^2}+\left(\frac{\eta\mu'(z)+\frac{\hat{P}'(z)}{2}-\frac{\hat{\rho}g}{2}}{\eta\mu(z)+\frac{\hat{P}(z)}{2}-\frac{\hat{\rho}gz}{2}}\right)\frac{d\psi_{30}(z)}{dz}\\&=\frac{k^2\left(\eta\mu(z)-\frac{\hat{\rho}gz}{2}\right)}{\left(\eta\mu(z)+\frac{\hat{P}(z)}{2}-\frac{\hat{\rho}gz}{2}\right)}\left\{1-\frac{\hat{\rho}c^2}{\left(\eta\mu(z)-\frac{\rho gz}{2}\right)}\right\}\psi_{30}(z)\end{aligned}\quad(41)$$

Substituting $\psi_{30}(z)=\psi_{31}(z)\Big/\sqrt{\eta\mu(z)+\frac{\hat{P}(z)}{2}-\frac{\hat{\rho}gz}{2}}$ in Eq. (41), and using Eq. (37) one may get

$$\begin{aligned}&\frac{d^2\psi_{31}}{dz^2}+\frac{\frac{1}{4}\left\{\eta\mu_3\alpha+\frac{(P_3\beta-g\rho_3)}{2}\right\}^2}{\left\{\eta\mu_3(1+\alpha z)+\frac{P_3+(P_3\beta-g\rho_3)z}{2}\right\}^2}\psi_{31}(z)\\&-\frac{k^2\left(\eta\mu_3(1+\alpha z)-\frac{\rho_3gz}{2}\right)}{\left\{\eta\mu_3(1+\alpha z)+\frac{P_3+(P_3\beta-g\rho_3)z}{2}\right\}}\\&\times\left\{1-\frac{\rho_3c^2}{\left(\eta\mu_3(1+\alpha z)-\frac{\rho_3gz}{2}\right)}\right\}\psi_{31}(z)=0\end{aligned}\quad(42)$$

Again, using a transformation $\psi_{31}(z)=\psi_{32}(\chi)$, where $\chi=\frac{2k\left\{\eta\mu_3(1+\alpha z)+\frac{P_3+(P_3\beta-g\rho_3)z}{2}\right\}}{\left\{\eta\mu_3\alpha+\frac{(P_3\beta-g\rho_3)}{2}\right\}}$ in Eq. (42), following form may be instated

$$\frac{d^2\psi_{32}(\chi)}{d\chi^2}+\left\{\frac{1}{4\chi^2}+\frac{\text{A}}{\chi}-\hbar\right\}\psi_{32}(\chi)=0\quad(43)$$

where

$$\text{A}=\frac{\frac{P_3}{2\mu_3}+\frac{c^2}{c_3^2}}{2\left\{\frac{\eta\alpha}{k}+\frac{1}{2}\left(\frac{P_3}{\mu_3}\frac{\beta}{k}-G\right)\right\}}-\frac{\frac{P_3}{4\mu_3}\frac{\beta}{k}\left(\eta+\frac{P_3}{2\mu_3}\right)}{\left\{\frac{\eta\alpha}{k}+\frac{1}{2}\left(\frac{P_3}{\mu_3}\frac{\beta}{k}-G\right)\right\}^2},$$

$$\hbar=\frac{1}{4}-\frac{\frac{P_3}{4\mu_3}\frac{\beta}{k}}{\left\{\frac{\eta\alpha}{k}+\frac{1}{2}\left(\frac{P_3}{\mu_3}\frac{\beta}{k}-G\right)\right\}}\text{ and }G=\frac{g\rho_3}{\mu_3k}$$

is Biot's gravity parameter and $c_3=\sqrt{\mu_3/\rho_3}$ is the shear wave velocity in the dry sandy half space.

Eq. (43) is the famous Whittaker equation, and as the solution of Eq. (43) must be confined and fades away for large distance from the boundary surface i.e., at $z\to\infty$

for the surface wave imply $\chi \to \infty$, appropriate solution may be taken as

$$\psi_{32}(\chi) = Y_5 W_{\frac{A}{2\sqrt{\hbar}},0}(2\sqrt{\hbar}\chi)$$

where Y_5 is arbitrary constant and $W_{\frac{A}{2\sqrt{\hbar}},0}(2\sqrt{\hbar}\chi)$ is the Whittaker function (Whittaker and Watson (1991)).

Considering Whittaker function unto linear phrase, we get the displacement for the torsional surface wave in the lower half space as

$$v_3(r,z,t) = \frac{Y_5 e^{-\sqrt{\hbar}\chi}\left(2\sqrt{\hbar}\chi\right)^{\frac{A}{2\sqrt{\hbar}}}}{\sqrt{\eta\mu_3\left(1+\alpha z\right)+\frac{1}{2}\left\{P_3+\left(P_3\beta-g\rho_3\right)z\right\}}} \times\left\{1-\frac{\left(\frac{A}{2\sqrt{\hbar}}-\frac{1}{2}\right)^2}{2\sqrt{A}\chi}\right\}J_1(kr)e^{i\omega t} \tag{44}$$

4. Boundary conditions and secular equation

The geometry of the problem proceeds to the consequent conditions:

(I) On the free surface, $z=-H_2$ of the topmost layer (M_1), the shear stress is zero, so that

(i) $\tau_{\theta z}^{(1)}=0$, at $z=-H_2$, (fluid saturated porous layer) (45a)

(ii) $\tau_{\theta z}^{(2)}=0$, at $z=-H_2$, (transversely isotropic layer) (45b)

(II) As the width of the intermediate fiber reinforced layer (M_2) is H_1 and it is supposed that, wave is continuous at the boundary surface of the media, i.e., at $z=-H_1$, the velocity of the topmost layer (M_1), is equal velocity of the fiber reinforced layer (M_2) and also stress is same from either side. Mathematically, boundary conditions at $z=-H_1$, are

(i) $v_{1F}=v_2$, i.e., displacement components are continuous (fluid saturated porous layer and fiber composite layer). (46a)

(ii) $v_{1T}=v_2$, i.e., displacement components are continuous (transversely isotropic layer and fiber composite layer). (46b)

and

(iii) $\tau_{\theta z}^{(1)}=\bar{\sigma}_{\theta z}$, i.e., stress components are continuous (fluid saturated porous layer and fiber composite layer). (47a)

(iv) $\tau_{\theta z}^{(2)}=\bar{\sigma}_{\theta z}$, i.e., stress components are continuous (transversely isotropic layer and fiber composite layer). (47b)

(III) Again at $z=0$, the common surface of the fiber reinforced composite layer (M_2) and the dry-sandy substrate (M_3), the displacement component is continuous and stress of fiber reinforced layer and dry-sandy half space are equal. In terms of mathematics, boundary conditions at $z=0$, may be written as

(i) $v_2=v_3$, i.e., displacement components are continuous. (fiber composite layer and dry Sandy substratum). (48)

(ii) $\bar{\sigma}_{\theta z}=\hat{\pi}_{z\theta}$, i.e., stress components are continuous. (fiber composite layer and dry Sandy substratum). (49)

Using the preceding boundary conditions with the help of Eq. (19), Eq. (25), Eq. (35), and Eq. (44) we get

$$Y_{11}e^{\Omega_F H_2}-Y_{21}e^{-\Omega_F H_2}=0 \tag{50a}$$

$$Y_{12}e^{\Omega_T H_2}-Y_{22}e^{-\Omega_T H_2}=0 \tag{50b}$$

$$Y_{11}e^{\Omega_F H_1}+Y_{21}e^{-\Omega_F H_1}+Y_3 e^{\tilde{M}H_1/2}\sin\left(qH_1\right)-Y_4 e^{\tilde{M}H_1/2} \times\cos\left(qH_1\right)=0 \tag{51a}$$

$$Y_{12}e^{\Omega_T H_1}+Y_{22}e^{-\Omega_T H_1}+Y_3 e^{\tilde{M}H_1/2}\sin\left(qH_1\right)-Y_4 e^{\tilde{M}H_1/2} \times\cos\left(qH_1\right)=0 \tag{51b}$$

$$Y_{11}\Omega_F L_1 e^{\Omega_F H_1}-Y_{21}\Omega_F L_1 e^{-\Omega_F H_1}-Y_3 e^{\tilde{M}H_1}\left\{-\sin\left(qH_1\right) \times\tilde{M}\tilde{R}/2-q\tilde{R}\cos\left(qH_1\right)+\tilde{Q}J\sin\left(qH_1\right)\right\}-Y_4 e^{\tilde{M}H_1} \times\left\{\cos\left(qH_1\right)\tilde{M}\tilde{R}/2-q\tilde{R}\sin\left(qH_1\right)-\tilde{Q}J\cos\left(qH_1\right)\right\}=0 \tag{52a}$$

$$Y_{12}\Omega_T c_{66}e^{\Omega_T H_1}-Y_{22}\Omega_T c_{66}e^{-\Omega_T H_1}-Y_3 e^{\tilde{M}H_1}\left\{-\sin\left(qH_1\right) \times\tilde{M}\tilde{R}/2-q\tilde{R}\cos\left(qH_1\right)+\tilde{Q}J\sin\left(qH_1\right)\right\}-Y_4 e^{\tilde{M}H_1} \times\left\{\cos\left(qH_1\right)\tilde{M}\tilde{R}/2-q\tilde{R}\sin\left(qH_1\right)-\tilde{Q}J\cos\left(qH_1\right)\right\}=0 \tag{52b}$$

$$Y_4=Y_5\,\Phi_1(\text{say}) \tag{53}$$

and

$$Y_3 q\tilde{R}+Y_4\left(-\tilde{M}\tilde{R}/2+\tilde{Q}J\right)=Y_5\,\Phi_2\,(\text{say}) \tag{54}$$

Eliminating the arbitrary constants Y_{11}, Y_{21}, Y_3, Y_4 and Y_5 from the above five equations, Eq. (50a), Eq. (51a), Eq. (52a), Eq. (53) and Eq. (54), and hence simplifying the obtained relation gets secular equation (dispersion equation) of torsional surface wave in an initially stressed fiber reinforced medium confined within initially stressed fluid saturated porous layer and initially stressed dry-sandy half space (for case-I) as

$$\tan\left(qH_1\right)=\frac{X_1+X_2\tan\left\{\Omega_F^*\left(H_2-H_1\right)\right\}}{X_3+X_4\tan\left\{\Omega_F^*\left(H_2-H_1\right)\right\}} \tag{55}$$

Similarly, eliminating the arbitrary constants Y_{12},Y_{22},Y_3,Y_4 and Y_5 from the above five equations, Eq. (50b), Eq. (51b), Eq. (52b), Eq. (53) and Eq. (54), and hence simplifying the obtained relation gets dispersion equation of torsional surface wave in an initially stressed fiber reinforced medium confined within initially stressed transversely isotropic layer and initially stressed dry-sandy half space (for case-II) as

$$\tan\left(qH_1\right)=\frac{X_1+X_5\tan\left\{\Omega_T^*\left(H_2-H_1\right)\right\}}{X_3+X_6\tan\left\{\Omega_T^*\left(H_2-H_1\right)\right\}} \tag{56}$$

where $\Omega_F^*,\Omega_T^*,\Phi_1,\Phi_2,X_j(j=1,..,6)$ are given in the Appendix A.

4.1 Special cases

When uppermost layer makes homogeneous and perfectly elastic (i.e., the directional rigidities and density reduces to constant) and free from initial stress for both the cases (i.e., for case-I, $N_1=L_1=\mu_{1F},\kappa\to1,P_{1F}\to0$ and for case-II, $c_{11}=\lambda_1+2\mu_{1T},c_{12}=\lambda_1,c_{55}=2\mu_{1T},P_{1T}\to0$) then dispersion equation, Eq. (55) & Eq. (56) takes the form respectively as

$$\tan\left(qH_1\right)=\frac{X_{11}+X_{21}\tan\left\{\tilde{\Omega}_F^*\left(H_2-H_1\right)\right\}}{X_{31}+X_{41}\tan\left\{\tilde{\Omega}_F^*\left(H_2-H_1\right)\right\}}\quad\text{and}$$

$$\tan\left(qH_1\right)=\frac{X_{11}+X_{51}\tan\left\{\tilde{\Omega}_T^*\left(H_2-H_1\right)\right\}}{X_{31}+X_{61}\tan\left\{\tilde{\Omega}_T^*\left(H_2-H_1\right)\right\}}$$

where $X_{j1}(j=1,..,6),\tilde{\Omega}_F^*$ and $\tilde{\Omega}_T^*$ are given in the Appendix B.

When uppermost layer makes homogeneous and perfectly elastic (i.e., the directional rigidities and density reduces to constant) and free from initial stress for both the cases (i.e., for case-I, $N_1=L_1=\mu_{1F},\kappa\to1,P_{1F}\to0$ and for case-II, $c_{11}=\lambda_1+2\mu_{1T},c_{12}=\lambda_1,c_{55}=2\mu_{1T},P_{1T}\to0$) and intermediate layer is without reinforcement and free from initial stress, isotropic elastic (i.e., $f_L=f_T=\mu_2;$ $\varsigma_1,\varsigma_3,P_2\to0$) then dispersion equation, Eq. (55) and Eq. (56) takes the form respectively as

$$\tan\left(\tilde{q}H_1\right)=\frac{X_{12}+X_{22}\tan\left\{\tilde{\Omega}_F^*\left(H_2-H_1\right)\right\}}{X_{32}+X_{42}\tan\left\{\tilde{\Omega}_F^*\left(H_2-H_1\right)\right\}}\quad\text{and}$$

$$\tan\left(\tilde{q}H_1\right)=\frac{X_{12}+X_{52}\tan\left\{\tilde{\Omega}_T^*\left(H_2-H_1\right)\right\}}{X_{32}+X_{62}\tan\left\{\tilde{\Omega}_T^*\left(H_2-H_1\right)\right\}}$$

where $X_{j2}(j=1,..,6),\tilde{\Omega}_F^*,\tilde{\Omega}_T^*$ and $\tilde{q}$ are given in the Appendix B.

When uppermost layer makes homogeneous and perfectly elastic (i.e., the directional rigidities and density becomes constant) and free from initial stress for both the cases (i.e., for case-I, $N_1=L_1=\mu_{1F},\kappa\to1,P_{1F}\to0$ and for case-II, $c_{11}=\lambda_1+2\mu_{1T},c_{12}=\lambda_1,c_{55}=2\mu_{1T},P_{1T}\to0$) and intermediate layer is without reinforcement and free from initial stress, isotropic elastic (i.e., $\varsigma_1,\varsigma_3,P_2\to0,f_L=f_T=\mu_2$) and lowermost half-space is isotropic homogeneous elastic, without initial stress and free from gravity (i.e., inhomogeneity parameters are all zero and $\eta\to1,T\to\mu_3;\alpha,\beta,g,P_3\to0$) then dispersion equation, Eq. (55) & Eq. (56) takes the form respectively as

$$\mu_2\tilde{q}\tan\left(\tilde{q}H_1\right)+\tilde{\Omega}_F^*\mu_{1F}\tan\left\{\tilde{\Omega}_F^*\left(H_2-H_1\right)\right\}=0\quad\text{and}$$

$$\mu_2\tilde{q}\tan\left(\tilde{q}H_1\right)+\tilde{\Omega}_T^*\mu_{1T}\tan\left\{\tilde{\Omega}_T^*\left(H_2-H_1\right)\right\}=0$$

where $\tilde{\Omega}_F^*,\tilde{\Omega}_T^*$ and $\tilde{q}$ are given in the appendix-B.

When uppermost layer is initially stressed fluid saturated porous layer (for case-I) or initially stressed transversely isotropic (for case-II) and intermediate layer is initially stressed fiber reinforced and lowermost half space is isotropic homogeneous elastic, without initial stress and free from gravity (i.e., $\eta\to1,T\to\mu_3,\alpha,\beta,g,P_3\to0$) then dispersion equation, Eq. (55) & Eq. (56) takes the form respectively as

$$\tan\left(qH_1\right)=\frac{X_{14}+X_{24}\tan\left\{\Omega_F^*\left(H_2-H_1\right)\right\}}{X_{34}+X_{44}\tan\left\{\Omega_F^*\left(H_2-H_1\right)\right\}}\quad\text{and}$$

$$\tan\left(qH_1\right)=\frac{X_{14}+X_{54}\tan\left\{\Omega_T^*\left(H_2-H_1\right)\right\}}{X_{34}+X_{64}\tan\left\{\Omega_T^*\left(H_2-H_1\right)\right\}}$$

in which $X_{j4}(j=1,..,6),\Omega_F^*,\Omega_T^*$ are given in the Appendix B.

When uppermost layer is initially stressed fluid saturated porous (for case-I) or initially stressed transversely isotropic (for case-II) and intermediate layer is without reinforcement and free from initial stress, isotropic elastic (i.e., $f_L=f_T=\mu_2;\varsigma_1,\varsigma_3,P_2\to0$) and lowermost half space is isotropic homogeneous elastic, without initial stress and free from gravity (i.e., $\eta\to1,T\to\mu_3,\ \alpha,\beta,g,P_3\to0$), then dispersion equation, Eq. (55) and Eq. (56) takes the form respectively as

$$\tilde{q}\tilde{R}\tan\left(\tilde{q}H_1\right)+k\mu_3+\Omega_F^*L_1\tan\left\{\tilde{\Omega}_F^*\left(H_2-H_1\right)\right\}=0\quad\text{and}$$

$$\tilde{q}\tilde{R}\tan\left(\tilde{q}H_1\right)+k\mu_3+\Omega_T^*c_{66}\tan\left\{\Omega_T^*\left(H_2-H_1\right)\right\}=0$$

in which Ω_F^*,Ω_T^* and $\tilde{q}$ are given in the appendix-B.

When uppermost layer is initially stressed free fluid saturated porous (for case-I) or initially stressed free transversely isotropic (for case-II) and intermediate layer is without reinforcement and free from initial stress, isotropic elastic (i.e., $f_L=f_T=\mu_2;\ \varsigma_1,\varsigma_3,P_2\to0$) and lowermost dry sandy half space is without initial stress and free from gravity (i.e., $g,P_3\to0$) then dispersion equation, Eq. (55) and Eq. (56) takes the form respectively as

$$\tan\left(\tilde{q}H_1\right)=\frac{X_{16}+X_{26}\tan\left\{\bar{\Omega}_F^*\left(H_2-H_1\right)\right\}}{X_{36}+X_{46}\tan\left\{\bar{\Omega}_F^*\left(H_2-H_1\right)\right\}}\quad\text{and}$$

$$\tan\left(\tilde{q}H_1\right)=\frac{X_{16}+X_{56}\tan\left\{\bar{\Omega}_T^*\left(H_2-H_1\right)\right\}}{X_{36}+X_{66}\tan\left\{\bar{\Omega}_T^*\left(H_2-H_1\right)\right\}}$$

in which $X_{j6}(j=1,..,6),\bar{\Omega}_F^*,\bar{\Omega}_T^*,\tilde{q}$ are given in the appendix-B.

When intermediate layer is absent {i.e., $H_1\to 0$ } and uppermost layer is homogeneous and perfectly elastic and free from initial stress for both the cases (i.e., for case-I, $N_1=L_1=\mu_{1F},\kappa\to 1,P_{1F}\to 0$ and for case-II, $c_{11}=\lambda_1+2\mu_{1T},c_{12}=\lambda_1,c_{55}=2\mu_{1T},P_{1T}\to 0$) and lowermost half-space is isotropic homogeneous elastic, without initial stress and free from gravity (i.e., inhomogeneity parameters are all zero and $\eta\to 1,T\to\mu_3;\alpha,\beta,g,P_3\to 0$) then the dispersion equation, for case-I, Eq. (55), & for case-II, Eq. (56) and takes the form respectively as

$$\tan\left(kH_2\sqrt{\frac{c^2}{c_{1F}^2}-1}\right)=\left(\mu_3\sqrt{1-\frac{c^2}{c_3^2}}\right)\Bigg/\left(\mu_{1F}\sqrt{\frac{c^2}{c_{1F}^2}-1}\right)$$

and

$$\tan\left(kH_2\sqrt{\frac{c^2}{c_{1T}^2}-1}\right)=\left(\mu_3\sqrt{1-\frac{c^2}{c_3^2}}\right)\Bigg/\left(\mu_{1T}\sqrt{\frac{c^2}{c_{1T}^2}-1}\right)$$

which is a widely known classical dispersion result of Love wave in a homogeneous layer laying over an isotropic homogeneous half space and hence affirming the problem discussed.

When topmost layer is absent {i.e., $H_2\to H_1$ }, intermediate layer is without reinforcement and free from initial stress, isotropic elastic (i.e., $\varsigma_1=\varsigma_3=0,$ $f_L=f_T=\mu_2,P_2\to 0$) and lowermost half space is isotropic homogeneous elastic, without initial stress and free from gravity (i.e., inhomogneity parameters are all zero and $\eta\to 1,T\to\mu_3,\alpha,\beta,g,P_3\to 0$) then the dispersion equation, Eq. (55) & Eq. (56) both takes the form

$$\tan\left(kH_1\sqrt{\frac{c^2}{c_2^2}-1}\right)=\left(\mu_3\sqrt{1-\frac{c^2}{c_3^2}}\right)\Bigg/\left(\mu_2\sqrt{\frac{c^2}{c_2^2}-1}\right)$$

which is a widely known classical dispersion result of Love wave in a homogeneous layer laying over an isotropic homogeneous half space and hence affirming the problem discussed.

5. Numerical computation and discussion

In order to realize the impact of numerous parameters viz. reinforcement, sandy parameter, Biot's gravity parameter, initial stresses, porosity, width ratio of the layers and other inhomogeneity parameters coupled with layers and half space and for the intent of numerical computation of nondimensionlize phase velocity of torsional surface wave generating in an initially stressed fiber reinforced layer, sandwiched between initially stressed porous layer (for case-I) or initially stressed transversely isotropic layer (for case-II) and a gravitating dry sandy substratum subjected to initial stress, we presumed the following data:

For uppermost initially stressed fluid saturated homogeneous layer (M_1) (for case-I): (Samal and Chattaraj (2011)) (Water-Saturated lime stone)

$N_1=2.774\times10^9\ N/m^2, L_1=1.387\times10^9\ N/m^2,$

$\hat{\Theta}=0.26,\rho_{rr}=1926.137\,kg/m^3,$

$\rho_{r\theta}=2.137\,kg/m^3,\rho_{\theta\theta}=215.337\,kg/m^3$

where N_1,L_1 represents shear moduli, $\hat{\Theta}$ is the porosity and $\rho_{rr},\rho_{r\theta},\rho_{\theta\theta}$ are densities of the layer, the solid and the liquid respectively.

For uppermost initially stressed transversely isotropic layer (M_1) (for case-II): (Prosser and Green Jr (1990)) (T300/5208 graphite/epoxy material)

$c_{11}=14.26\times10^9\ N/m^2, c_{12}=6.78\times10^9\ N/m^2,$

$c_{55}=5.27\times10^9\ N/m^2,\rho_{1T}=1422\,kg/m^3$

where c_{11}, c_{12}, c_{55} are elastic constants and ρ_{1T} is the density of the transversely isotropic solid.

For intermediate, initially stressed fiber reinforced layer (M_2): (Markham (1969)) (Carbon fiber-epoxy resin)

$f_L=5.66\times10^9\ N/m^2, f_T=2.46\times10^9\ N/m^2,$

$\rho_2=1671kg/m^3$

where f_L, f_T are transversal shear modulus and longitudinal shear modulus respectively and ρ_2 is the density of the sandwiched layer.

For initially stressed anisotropic gravitating dry-sandy half space (M_3): (Gubbins 1990) (Anisotropic sandstone material)

$\mu_3=65.4\times10^9\ N/m^2,\ \rho_3=3409\,kg/m^3$

where μ_3 are rigidity and ρ_3 is the density of the half space.

The figures have been constructed by assuming the vertical axis as a dimensionless phase velocity (c/c_2) versus horizontal axis as a dimensionless wave number kH_1 . For graphical illustration, we have taken the fixed values of the parameters as

$\kappa=0.90,\ \xi_{1F}=0.2,\ \xi_{1T}=0.2,\ \xi_2=0.3,\ \alpha/k=0.5,$ $\beta/k=0.2,\ \eta=1.05,\ G=1.0,\ \xi_3=0.3$ and $H=2.0$; unless the varying values shown in the respective figures. Here $\xi_{1F}=P_{1F}/2L_1,\ \xi_{1T}=P_{1T}/2c_{55},\ \xi_2=P_2/2f_T$, $\xi_3=P_3/2\mu_3,\ H=H_2/H_1$ and also in all the figures solid and dashed curves represent Case-I and Case-II respectively.

Moreover, the following data have also been used, $kr=3.5,\ \upsilon=60^0,$ i.e., $\varsigma_1=\sqrt{3}/2,\ \varsigma_2=0,\ \varsigma_3=1/2$ and we take asymptotic expansion of Bessel function of first kind with order one up to five terms.

Here the following cases may be discussed for fluid saturated porous medium,

(i) For porous layer, if $\hat{\Theta}\to 1$ then $\rho_f\to\hat{\rho}$, thus the bulk material becomes fluid i.e., $\phi_{11}-\phi_{12}^2/\phi_{22}\to 0$, or $\kappa\to 0$. It represents shear waves does not exist.

(ii) For non-porous layer, if $\kappa\to 0$ and $\rho_s\to\hat{\rho}$

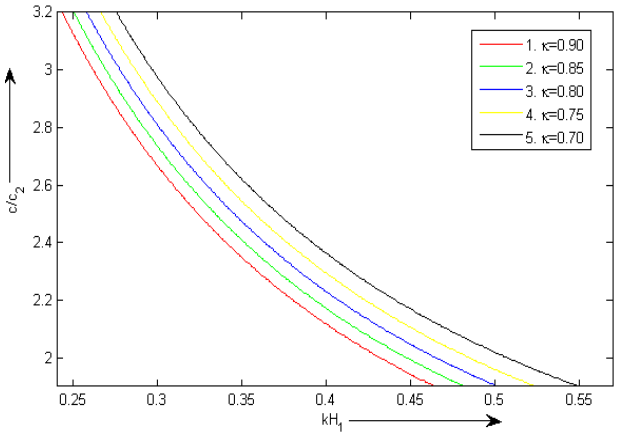

Fig. 2 Variation of the dimensionless phase velocity (c/c_2) versus the non-dimensional wave number kH_1 for different values of porosity parameter (κ) (Case–I)

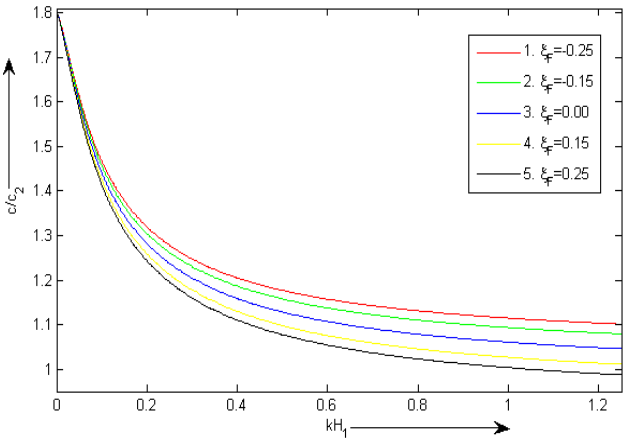

Fig. 3 Variation of the dimensionless phase velocity (c/c_2) against the non-dimensional wave number kH_1 for various values of initial stress parameter (ξ_{1F}) (Case–I)

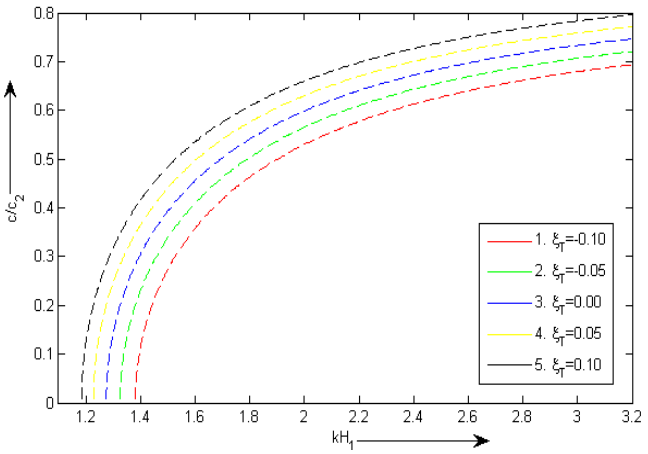

Fig. 4 Variation of the dimensionless phase velocity (c/c_2) against the non-dimensional wave number kH_1 for different values of initial stress parameter (ξ_{1T}) (Case–II)

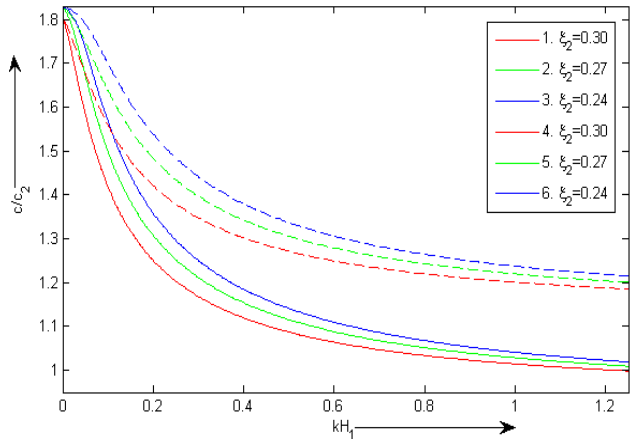

Fig. 5 Variation of the dimensionless phase velocity (c/c_2) versus the non-dimensional wave number kH_1 for various values of initial stress parameter (ξ_2)

which proceeds to $\phi_{11}+\phi_{12}\to 1$ and $\phi_{12}+\phi_{22}\to 0$, which gives to $\phi_{11}-\phi_{12}^2/\phi_{22}\to 1$ or $\kappa\to 1$. Thus, for porous substrate $0<\kappa<1$.

Fig. 2 depicts the consequence of porosity parameter (κ) for different values, associated with upper poro-elastic medium (case-I). In Fig. 2, the values of (κ) for curves 1, 2, 3, 4, and 5, respectively have been taken as 0.90, 0.85, 0.80, 0.75 and 0.70. From these figures, it has been observe that as the porosity of the layer decreases, the phase velocity (c/c_2) of the torsional wave number increases for a certain wave number kH_1. Result points out that porosity (κ) of the layer is inversely proportionate to the phase velocity (c/c_2) of the torsional surface wave. The curves that are uniformly away from each other shows the prominant effect of the porosity on torsional wave propagation.

Fig. 3 decorate the notable influence of horizontal initial stress (case-I) on the phase velocity of a torsional surface. When $\xi_{1F}>0$, it is designated compressive initial stress, whereas when $\xi_{1F}<0$, is yclept tensile initial stress. To show effect of compressive and tensile stresses, values of ξ_{1F} for curves 1, 2, 3, 4 and 5, have been taken as -0.25, -0.15, 0.0, 0.15, 0.25 respectively. It has been noticed that as the value of (ξ_{1F}) increases, the phase velocity decreases at a certain wave number. The impact has egress more conspicuously at lower wave number.

Fig. 4 describes the domination of horizontal initial stress (ξ_{1T}) parameter (case-II) for distinct values. This case is almost similar to previous one. To show effect of compressive and tensile stresses, values of (ξ_{1T}) for curves 1, 2, 3, 4 and 5, respectively have been assume as -0.1, -0.05, 0.0, 0.05, and 0.1. It has been perceived that as the value of (ξ_{1T}) increases, the phase velocity increases uniformly at a fixed wave number.

Fig. 5 depicts the effect of the initial compressive stress parameter (ξ_2) associated with the intermediate layer on the phase velocity (c/c_2) of the torsional surface wave. The

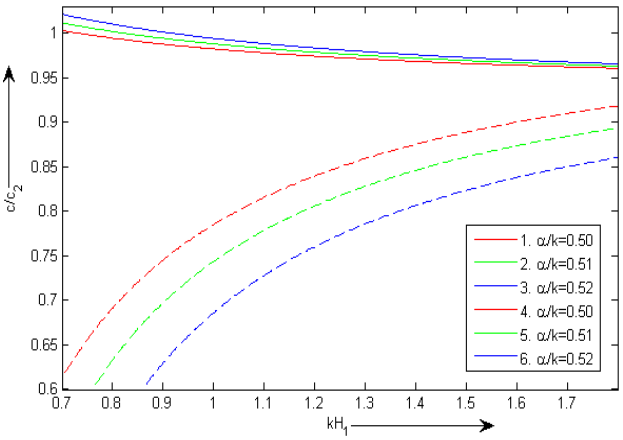

Fig. 6 Variation of the dimensionless phase velocity (c/c_2) against the non-dimensional wave number kH_1 for different values of inhomogeneity parameter (α/k)

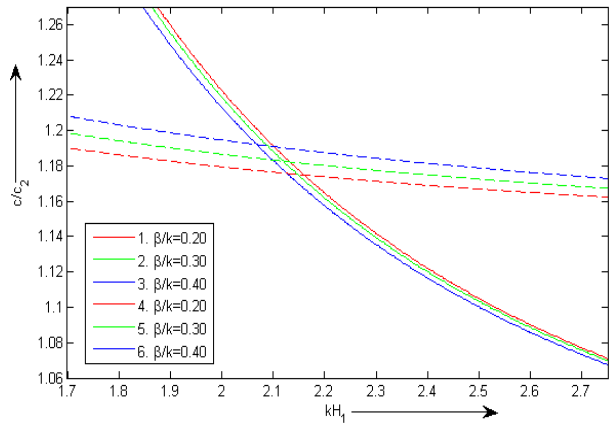

Fig. 7 Variation of the dimensionless phase velocity (c/c_2) against the non-dimensional wave number kH_1 for various values of inhomogeneity parameter (β/k)

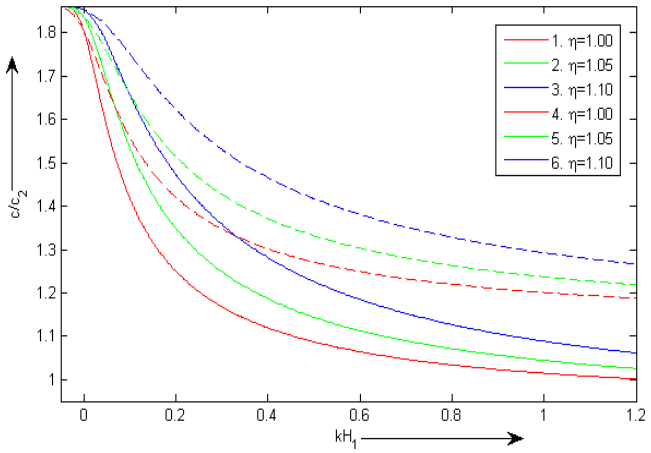

Fig. 8 Variation of the dimensionless phase velocity (c/c_2) versus the non-dimensional wave number kH_1 for various values of sandy parameter (η)

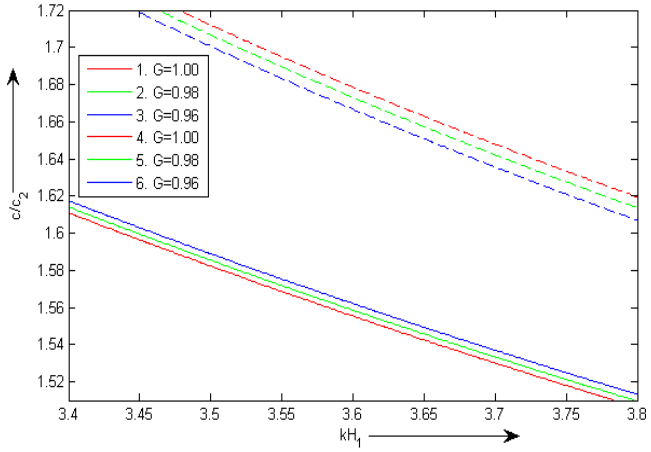

Fig. 9 Variation of the dimensionless phase velocity (c/c_2) versus the non-dimensional wave number kH_1 for various values of Biot's gravity parameter (G)

values of (ξ_2) are taken as 0.3, 0.27, and 0.24 for Curves 1, 2, and 3, respectively for case-I and Curves 4, 5, and 6, respectively for case-II. Fig. 5 demonstrates that the phase velocity raises as decline in the dimension less wave number and ratifies that as the compressive initial stress parameter increases, the phase velocity of the torsional type surface wave decreases. In the absence of initial stress, highest phase velocity has been detected and it validates noticeable effect of initial stress on wave propagation.

Fig. 6 signifies the dispersion curve of the torsional surface wave subjected to inhomogeneity parameter (α/k) conjoined in the rigidity of the dry Sandy Gibson half space. The values of (α/k) are taken as 0.50, 0.51, and 0.52 for Curves 1, 2, and 3, respectively for case-I and Curves 4, 5, and 6, respectively for case-II. Figure 6 shows that the velocity of the torsional type surface wave recedes (case-I) and increases (case-II) with increment in the wave number kH_1, which reaffirms that the phase velocity (c/c_2) increases (case-I) and decreases (case-II) with an increase in the inhomogeneity parameter (α/k) of the half space, for fixed values of wave number kH_1.

Fig. 7 delineates the impact of inhomogeneity parameter (β/k). The values of (β/k) are taken as 0.20, 0.30, and 0.40 for curves 1, 2, and 3, respectively for case-I and Curves 4, 5, and 6, respectively for case-II. From figure it can be seen that the phase velocity reduce (case-I) and increases (case-II) with the increasing values of inhomogeneity parameters. In comparison to above two cases, minimum impact of inhomogeneity parameters $\{\alpha/k, \beta/k\}$ has been found in case-I.

Fig. 8 signifies the impression of the sandy parameter (η) on the phase velocity of the wave for individual values of (η) under the influence of initial stress. The value of (η) for Curves 1, 2, and 3, respectively for case-I and Curves 4, 5, and 6, respectively for case-II, are considered as 1.00, 1.05, and 1.10 respectively. The graph gives the

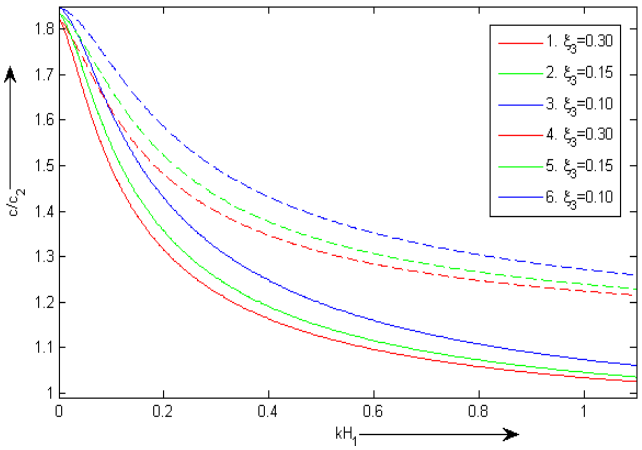

Fig. 10 Variation of the dimensionless phase velocity (c/c_2) against the non-dimensional wave number kH_1 for different values of initial stress parameter (ξ_3)

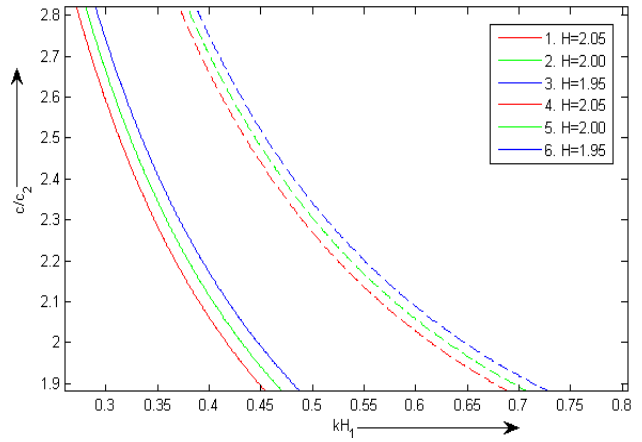

Fig. 11 Variation of the dimensionless phase velocity (c/c_2) versus the non-dimensional wave number kH_1 for various values of ratio of thickness of layers (H)

clear picture of initial stress, for a particular value of non-dimensional wave number kH_1, for both the cases, the phase velocity (c/c_2) increases as the value of sandiness (η) increases.

Fig. 9 manifests the consequence of gravity on the generation of the torsional surface wave in the half space. The value of (G)for curves 1, 2, and 3, respectively for case-I and Curves 4, 5, and 6, respectively for case-II, are considered as 1.0, 0.98, and 0.96 respectively. It has been found from the dispersion curves of present figure, that as the Biot's gravity parameter (G) of the half space decreases, the phase velocity increases remarkably (case-I) and decreases remarkably (case-II) at a fixed wave number thereby, it shows the phenomena that phase velocity of torsional surface wave is inversely proportional (case-I) and directly proportional (case-II) to the gravity of the dry sandy half space.

Fig. 10 depicts the effect of initial compressive stress (ξ_3) of the anisotropic Gibson half space on the dimensionless phase velocity (c/c_2) of torsional surface waves with variation in wave number kH_1 which provides the essence of having the influence of initial compressive stress in the half space detracts the phase velocity of torsional surface waves. In this figure, values of (ξ_3) are considered as 0.30, 0.15, and 0.10 for Curves 1, 2, and 3, respectively for case-I and Curves 4, 5, and 6, respectively for case-II. This figure highlights that the impact is approx. same as that of the Fig. 5, but the curves here are more apart from each other. Under these mentioned values, it can be observed that, as the compressive initial stress decreases, the dimensionless phase velocity (c/c_2) increases for a fixed wave number for both the cases. Thus, one can conclude that when half space is homogeneous then torsional surface wave is directly proportional to ξ_3 and increasing with same frequency as (ξ_3) increases.

Fig. 11 illustrates the consequence of thickness ratio (H) of the upper and intermediate layer. The value of (H) for curves 1, 2, and 3 respectively for case-I and Curves 4, 5, and 6 respectively for case-II, are taken as 2.05, 2.00, and 1.95 respectively. We observe that as the ratio of thickness of the layers (H) recedes, the phase velocity (c/c_2) of torsional surface at a particular frequency of wave number kH_1 increases, which validates the fact that phase velocity of torsional surface wave is inversely proportional to the ratio of thickness of the layers and also the curves are more apart from each other show the remarkable effect of the ratio of thickness of the layer on torsional surface wave propagation.

6. Conclusions

In the present problem, a mathematical model is developed for analytical study on torsional wave generation in a fiber reinforced layer, constrained between different anelastic layer and gravitating semi-infinite sandy substratum. Based on the calculated results, the subsequent conclusions can be drawn:

• The comparative study in the Figs. 7-11 shows that phase velocity of torsional surface wave is detected to be greater, for fixed value of wave number, when the topmost layer is transversely isotropic as compared with the event when the superficial layer is fluid saturated homogeneous porous.

• In the presumed condition, the torsional waves are executed to be dispersive in nature, the phase velocity increases or decreases with increase in dimensionless wave number in all the graphs.

• Increase of heterogeneity owning to directional rigidity of the substratum the phase velocity increases (for case-I) and decreases (for case-II).

• The acquired secular relation for the torsional surface wave is detected to be well in compliance with the classical Love wave equation as a particular case of the problem, when effect of non-homogeneity parameters and pre-stress is neglected from the secular relation of the torsional waves and one of the upper layers vanishes.

• The common velocity of torsional wave increases (for

case-I) and decreases (for case-II) as the Biot's gravity parameter (G) decreases, significantly.

• Existence of sandiness (η) in the half space increases the wave length of the torsional wave which bars the extension of seismic energy despatched through the sandy medium.

• It has been found that, the torsional surface wave transmits much slower and it indicates the effect of initial stress on phase velocity. The initial stresses staying in the anisotropic substratum, fiber reinforced medium and topmost anelastic medium also have a outstanding effect in the velocity of propagation.

• Present study manifest that the width of the layers performs a vital role in the analysis of torsional surface waves.

Acknowledgments

The authors convey their sincere thanks to Indian Institute of Technology (Indian School of Mines), Dhanbad, for facilitating us with its best facility for research.

References

Abo-El-Nour, N. and Alsheikh, F.A. (2009), "Reflection and refraction of plane quasi-longitudinal waves at an interface of two piezoelectric media under initial stresses", *Arch. Appl. Mech.*, **79**(9), 843-857.

Abo-El-Nour, N. and Abo-Dahab, S.M. (2008), "The influence of the viscosity and the magnetic field on reflection and transmission of waves at interface between magneto-viscoelastic materials", *Meccan.*, **43**(4), 437-448.

Ben-Hador, R. and Buchen, P. (1999), "Love and Rayleigh waves in non-uniform media", *Geophys. J. Int.*, **137**(2), 521-534.

Bhattacharya, R.C. (1975), "On the torsional wave propagation in a two-layered circular cylinder with imperfect bonding", *Proc. Ind. Natn. Sci. Acad.*, **41**(6), 613-619.

Biot, M.A. (1962), "Mechanics of deformation and acoustic propagation in porous media", *J. Appl. Phys.*, **33**(4), 1482-1489.

Biot, M.A. (1966), *Mechanics of Incremental Deformation*, Wiley, New York, U.S.A.

Bromwich, T.J. (1898), "On the influence of gravity on elastic waves, and, in particular, on the vibrations of an elastic globe", *Proc. Lond. Math. Soc.*, **30**, 98-120.

Carcione, J.M., Kosloff, D. and Kosloff, R. (1988), "Wave-propagation simulation in an elastic anisotropic (transversely isotropic) solid", *Quarter. J. Mech. Appl. Math.*, **41**, 319-346.

Chattaraj, R., Samal, S.K. and Mahanti, N.C. (2011), "Propagation of torsional surface wave in anisotropic poroelastic medium under initial stress", *Wave Mot.*, **48**, 184-195.

Chattopadhyay, A., Gupta, S., Samal, S.K. and Sharma, V.K. (2009), "Torsional wave in self-reinforced medium", *Int. J. Geomech.*, **9**, 9-13.

Chaudhary, S., Kaushik, V.P. and Tomar, S.K. (2005), "Transmission of shear waves through a self-reinforced layer sandwiched between two inhomogeneous viscoelastic half-spaces", *Int. J. Mech. Sci.*, **47**(9), 1455-1472.

Ding, H., Chen, W. and Zhang, L. (2006), *Elasticity of Transversely Isotropic Materials*, Springer Press, the Netherlands.

Gubbins, D. (1990), *Seismology and Plate Tectonics*, Cambridge University Press, Cambridge.

Gupta, S., Kundu, S., Pati, P. and Ahmed, M. (2018), "Torsional waves in fluid saturated porous layer clamped between two anisotropic media", *Geomech. Eng.*, **15**(1), 645-657.

Islam, Z.M., Jia, P. and Lim, C.W. (2014), "Torsional wave propagation and vibration of circular nanostructures based on nonlocal elasticity theory", *Int. J. Appl. Mech.*, **6**(2) 1450011, 1-17.

Kakar, R. (2015), "Torsional wave in an inhomogeneous prestressed elastic layer overlying an inhomogeneous elastic half-space under the effect of rigid boundary", *Earthq. Struct.*, **9**(4), 753-766.

Kakar, R. and Kakar, S. (2016), "Dispersion of shear wave in a pre-stressed hetrogeneous orthotropic layer over a pre-stressed anisotropic porous half-space with self-weight", *Struct. Eng. Mech.*, **59**(6), 951-972.

Kumar, S., Vishwakarma, S.K. and Gupta, S. (2013), "Existence of torsional surface waves in an earth's crustal layer lying over a sandy mantle", *J. Earth Syst. Sci.*, **122**, 1411-1421.

Kumari, P., Modi, C. and Sharma, V. K. (2016), "Torsional waves in a magneto-viscoelastic layer over an inhomogeneous substratum", *Eur. Phys. J. Plus*, **131**(8), 263.

Kundu, S., Alam, P. and Gupta, S. (2017), "Shear waves in magneto-elastic transversely isotropic (MTI) layer bonded between two heterogeneous elastic media", *Mech. Adv. Mater. Struct.*, 1-9.

Lata, P., Kumar, R. and Sharma, N. (2016), "Plane waves in an anisotropic thermoelastic", *Steel Compos. Struct.*, **22**, 567-587.

Manna, S., Kundu, S. and Gupta, S. (2015), "Effect of reinforcement and inhomogeneity on the propagation of Love waves", *Int. J. Geomech.*, **16**(2), 04015045.

Markham, M.F. (1969), "Measurements of Elastic constants of fibre composites by ultrasonics", *Compos.*, **1**(2), 145-149.

Meissner, E. (1921), "Elastische oberflächenwellen mit dispersion in einem inhomogenen medium", *Vierteljahresschrift der Naturforschenden Gesellschaft in Zürich*, **66**, 181-195.

Ozturk, A. and Akbarov, S.D. (2009), "Torsional wave propagation in a pre-stressed circular cylinder embedded in a prestressed elastic medium", *Appl. Math. Modell.*, **33**(9), 3636-3649.

Prosser, W.H. and Green Jr, R.E. (1990), "Characterization of the nonlinear elastic properties of graphite/epoxy composites using ultrasound", *J. Reinf. Plast. Compos.*, **9**, 162-173.

Sahu, S.A., Singh, M.K. and Pankaj, K.K. (2018), "Analysis of torsional waves in a prestressed composite structure with loosely bonded and corrugated boundaries", *Mech. Compos. Mater.*, **54**(3), 321-332.

Selim, M.M. (2010), "Torsional vibration of carbon nanotubes under initial compression stress", *Brazil. J. Phys.*, **40**(3), 283-287.

Sharma, V. and Kumar, S. (2016), "Influence of microstructure, heterogeneity and internal friction on SH waves propagation in a viscoelastic layer overlying a couple stress substrate", *Struct. Eng. Mech.*, **57**(4), 703-716.

Singh, A.K., Chaki, M.S., Hazra, B. and Mahto, S. (2017), "Influence of imperfectly bonded piezoelectric layer with irregularity on propagation of love-type wave in a reinforced composite structure", *Struct. Eng. Mech.*, **62**(3), 325-344.

Shekhar, S. and Parvez, I.A. (2016), "Propagation of torsional surface waves in a double porous layer lying over a Gibson half space", *Soil Dyn. Earthq. Eng.*, **80**, 56-64.

Son, M.S. and Kang, Y.J. (2012), "Propagation of shear waves in a poroelastic layer constrained between two elastic layers", *Appl. Math. Model.*, **36**, 3685-3695.

Spencer, A.J.M. (1972), *Deformations of Fiber-Reinforced Materials*, Oxford University Press, London, U.K.

Vinh, P.C., Aoudia, A. and Giang, P.T.H. (2016), "Rayleigh waves in orthotropic fluid-saturated porous media", *Wave Mot.*, **61**, 73-82.

Wang, Y.S. and Zhang, Z.M. (1998), "Propagation of Love waves in a transversely isotropic fluid saturated porous layered half-space", *J. Acoust. Soc. Am.*, **103**(2), 695-701.
Watanabe, K. (2014), "Reflection of an impulsive torsional wave by a moving boundary", *Wave Mot.*, **51**, 1209-1224.
Whittaker, E.T. and Watson, G.N. (1991), *A Course of Modern Analysis*, Cambridge University Press, Cambridge, U.K.

PL

Appendix A

$$X_1 = \frac{q\tilde{R}\mu_3\Phi_2}{k\Phi_1}, X_2 = \frac{\Omega_F^* L_1 q\tilde{R}}{k}, X_3 = \Psi_2\Psi_1 - \frac{q^2\tilde{R}^2}{k},$$

$$X_4 = \Omega_F^* L_1\Psi_1, X_5 = \frac{\Omega_T^* c_{55} q\tilde{R}}{k}, X_6 = \Omega_T^* c_{55}\Psi_1,$$

$$\Psi_1 = \frac{\mu_3\Phi_2}{k\Phi_1} - \frac{\Psi_2}{k}, \Psi_2 = \tilde{Q}J - \frac{\tilde{M}\tilde{R}}{2},$$

$$\Phi_1 = \frac{\Gamma e^{-\sqrt{\hbar}\chi_0}\left(2\sqrt{\hbar}\chi_0\right)^{\frac{\Lambda}{2\sqrt{\hbar}}}}{\sqrt{\eta\mu_3 + \frac{P_3}{2}}}, \ \Phi_2 = \Gamma\Bigg[-\frac{2e^{-\sqrt{\hbar}\chi_0}k\sqrt{\hbar}}{\sqrt{\eta\mu_3 + \frac{P_3}{2}}}$$

$$\times\left(2\sqrt{\hbar}\chi_0\right)^{\frac{\Lambda}{2\sqrt{\hbar}}} + \frac{2k\Lambda e^{-\sqrt{\hbar}\chi_0}}{\sqrt{\eta\mu_3 + \frac{P_3}{2}}}\left(2\sqrt{\hbar}\chi_0\right)^{\frac{\Lambda}{2\sqrt{\hbar}}-1} - \frac{1}{2}\frac{e^{-\sqrt{\hbar}\chi_0}}{\left(\eta\mu_3 + \frac{P_3}{2}\right)^{\frac{3}{2}}}$$

$$\times\left(2\sqrt{\hbar}\chi_0\right)^{\frac{\Lambda}{2\sqrt{\hbar}}}\left\{\eta\mu_3\alpha + \frac{P_3\beta - g\rho_3}{2}\right\}\Bigg], \ \Gamma = 1 - \frac{\left(\frac{\Lambda}{2\sqrt{\hbar}} - \frac{1}{2}\right)^2}{2\sqrt{\hbar}\chi_0},$$

$$\chi_0 = \lim_{z\to 0}\chi = \frac{4k\left(\eta\mu_3 + P_3\right)}{2\eta\mu_3\alpha + P_3\beta - g\rho_3}, \qquad J = \frac{kJ_1'(kr)}{J_1(kr)} - \frac{1}{r},$$

$$\Omega_F^* = i\Omega_F, \ \Omega_T^* = i\Omega_T, \quad \tilde{\Omega}_F^* = k\sqrt{\frac{c^2}{c_{1F}^2} - 1}, \ \tilde{\Omega}_T^* = k\sqrt{\frac{c^2}{c_{1T}^2} - 1}.$$

Appendix B

$$X_{11} = X_1, X_{21} = \tilde{\Omega}_F^* \mu_{1F} q\tilde{R}/k\,, X_{31} = X_3, X_{41} = \tilde{\Omega}_F^* \mu_{1F} \Psi_1,$$
$$X_{51} = \tilde{\Omega}_T^* \mu_{1T} q\tilde{R}/k\,, X_{61} = \tilde{\Omega}_T^* \mu_{1T} \Psi_1,$$
$$X_{12} = \frac{\tilde{q}\mu_2\mu_3\Phi_2}{k\Phi_1}, X_{22} = \frac{\tilde{\Omega}_F^* \mu_{1F}\tilde{q}\mu_2}{k}, X_{32} = -\frac{\tilde{q}^2\mu_2^2}{k},$$
$$X_{42} = \frac{\tilde{\Omega}_F^* \mu_{1F}\mu_3\Phi_2}{k\Phi_1}, X_{52} = \frac{\tilde{\Omega}_T^* \mu_{1T}\tilde{q}\mu_2}{k}, X_{62} = \frac{\tilde{\Omega}_T^* \mu_{1T}\mu_3\Phi_2}{k\Phi_1},$$
$$X_{14} = qk\tilde{R}\mu_3, X_{24} = \Omega_F^* L_1 q\tilde{R}, X_{34} = \Psi_2^2 + q^2\tilde{R}^2,$$
$$X_{44} = \Omega_F^* L_1 \Psi_2, X_{54} = \Omega_T^* c_{55} q\tilde{R}, X_{64} = \Omega_T^* c_{55}\Psi_2,$$
$$X_{16} = \tilde{q}\mu_2\mu_3\Upsilon^*, X_{26} = \frac{\tilde{q}\mu_2\bar{\Omega}_F^* L_1}{k}, X_{36} = -\frac{\tilde{q}^2\mu_2^2}{k},$$
$$X_{46} = \bar{\Omega}_F^* L_1\mu_3\Upsilon^*, X_{56} = \frac{\bar{\Omega}_T^* c_{55}\tilde{q}\mu_2}{k}, X_{66} = \bar{\Omega}_T^* c_{55}\mu_3\Upsilon^*$$
$$\tilde{q} = k\sqrt{\frac{J_1''(kr)}{J_1(kr)} + \frac{J_1'(kr)}{rkJ_1(kr)} + \frac{c^2}{c_2^2} - \frac{1}{(rk)^2}},$$
$$\bar{\Omega}_T^* = k\sqrt{\frac{(c_{11}-c_{12})}{k^2}\left\{\frac{kJ_1'(kr)}{2rc_{55}J_1(kr)} - \frac{1}{2r^2c_{55}}\right\} + \frac{(c_{11}-c_{12})J_1''(kr)}{2c_{55}J_1(kr)} + \frac{c^2}{c_{1T}^2}},$$
$$\bar{\Omega}_F^* = k\sqrt{\kappa\left(\frac{c}{c_{1F}}\right)^2\frac{N_1}{L_1} - \frac{N_1}{L_1}},$$
$$\Upsilon^* = -1 + \frac{c^2}{2\eta c_3^2} - \frac{\alpha}{2k} + \frac{\frac{1}{2}\left\{\frac{c^2k}{\eta\alpha c_3^2} - 1\right\}^2}{\frac{2k}{\alpha}\left[\frac{2k}{\alpha} - \frac{1}{2}\left\{\frac{c^2k}{\eta\alpha c_3^2} - 1\right\}^2\right]}.$$